Optical design and analysis of a head-mounted display with a high-resolution insert

Akitoshi Yoshida*, Jannick P. Rolland‡, and John H. Reif†

* Rechenzentrum der Universität Mannheim
D-68131 Mannheim, GERMANY

‡Department of Computer Science, University of North Carolina at Chapel Hill
Chapel Hill, NC 27599, USA

†Department of Computer Science, Duke University
Durham, NC 27708, USA

ABSTRACT

In a previous paper by the authors, a High-Resolution Insert Head-Mounted Display (HRI-HMD) that uses only fixed electronic devices was proposed and designed.[18] The design concept is innovative and it is the first and only known such design to implement a high-resolution insert for HMDs.

The high resolution insert system consists of three stages: an objective to collimate the image of the display, a duplicator to produce insert images, and an eyepiece to view the insert and background images. In this paper, a detailed description of the HRI-HMD is given, which includes detailed analysis of the performance and a discussion of physical constraints. Analysis is conducted for each stage as well as for the entire system. The potential benefits of individually optimizing each channel of the duplicator and balancing aberrations from different stages are discussed. The benefits of employing binary optics at the duplicator are also discussed. The geometry of a folded model is described as well. From this analysis, the achievable performance of the HRI-HMD can be estimated against its size and cost.

Keywords: Virtual Reality, Head-Mounted Display, Optical Design, Binary Optics

1. INTRODUCTION

The field of Virtual Reality (VR) has recently received considerable attention, due to the potential to create unique capabilities for human-computer interaction.[1,2] Such advanced interaction can include interactive control and diagnostics systems, educational and training systems, teleoperation systems, and entertainment systems.[3-8] For these applications, HMDs are typically used to provide visual information to the user;[9] however, conventional HMDs usually do not utilize the full potential of VR technology. In particular, they do not provide enough resolution or field of view to give the user the realistic feeling of being immersed in the computer-simulated virtual environment, nor support integrated effective interaction capabilities combining head and eye tracking.

For some applications, the feeling of being immersed in the computer-simulated world is critical for properly performing the required task. To give the user the feeling of immersion, two features of the HMD must be met. First, the display must provide a field of view large enough; second, it must provide resolution high enough to render the fine detail of the image. Too narrow of a field of view causes the user to see the frame of the display and to have the sense of looking through a window. To remove this perhaps annoying window effect, the field of view must be at least 80 degrees.[10,11] Too low of a resolution causes the user to see the individual pixels or raster scans of the display device and fine details of the image are lost. To match human visual acuity, the pixel size must be about 1 arc minute.[12] However, the human retina does not provide uniform visual acuity.[13,14] The high visual acuity is only available at the fovea, a small area of about 5° in angular extent at the center of the retina. The visual acuity degrades significantly as the distance from the fovea increases; at an angular distance of 5° from the center of the fovea, it is about a quarter of the highest acuity, and at an angular distance of 15°, it becomes only one seventh.[12] Therefore, the resolution does not have to be 1 arc minute over a large field.

For a fixed number of pixels in a display, these two features are contradictory. A large field of view leads to low resolution, and high resolution leads to a small field of view. Consequently, most HMDs do not provide these two features adequately. To overcome this dilemma, HMDs that combine a low-resolution, large-field background image with a high-resolution, small-field insert image have been developed.[15,16] Because of the property of the human visual system to have high visual acuity only over a narrow region around the fovea, a small area of high-resolution insert can be superposed on a large field of low-resolution image to virtually create a large field of view with high resolution. In this case, the position of the insert is dynamically controlled by the gaze point.

One approach taken originally by these systems was to use large high-resolution displays or light valves to generate the high-resolution insert and to use optics combined with a bundle of optical fibers to transport the images to the eyes. A more recent approach consists of using only one light valve and to render only the image at the gaze point more accurately than the surrounding image. These systems provide significant improvements over ordinary displays and are considered the best displays available, in spite of the fact that they are very heavy and extremely expensive. Moreover, it should be noticed that both of those approaches lead to a *non-portable* system.

Thus, currently available HMDs are either low-cost low-performance or high-cost high-performance models. Our approach is to develop an hybrid type, a low-cost high-performance insert HMD system that uses fully optoelectronic components. The use of fixed optoelectronic components allows the whole system to be fabricated with fewer alignment errors, to be immune to mechanical failure, to be generally more tolerant to vibrations, and most importantly to be portable.

The interaction capability currently integrated to HMDs is typically limited to the use of head tracking to measure the position and orientation of the user's head and to generate scenery from the user's perspective.[17] The user can navigate through the virtual world and interact with its objects by using three-dimensional manual input devices. For some situations which require very fast response time or difficult coordinated skills, interaction capability supported by such manual input devices becomes inadequate. For those cases, eye movement can be used in conjunction with manual input devices to provide effective fast and flexible interaction methods.

The basic concept of the HRI-HMD described in our previous paper[18] is to optically duplicate the insert image and to select one copy by blocking the other copies. The selected copy of the insert image is then optically superposed on the background image. The insert image traces the gaze point, thus the user sees the whole field at high resolution. The whole system can remain low-cost because it uses fixed optical components and ordinary display devices. The availability of such a low-cost high-performance HMD will significantly increase the potential of many virtual reality applications. In addition to the advantage of having a potentially large field of view and a high-resolution image, the HRI-HMD provides effective interaction methods through eye tracking. Thus, combined with appropriate computer software, the whole system will become an Active Vision HMD system that gives the user the feeling of being immersed in the virtual environment and provides effective gaze-point-oriented interaction methods.

In this paper, a design and analysis of the HRI-HMD is described in detail. The main component of the HRI-HMD is an optical system that positions the insert image over the background image. This component consists of three stages: an objective, a duplicator, and an eyepiece. The objective forms collimated light from the insert display; the duplicator forms an array of intermediate images from this collimated light; and finally the eyepiece forms collimated light from these images for viewing. To keep modularity, optical systems are independently designed for each stage. To investigate the optimal design, several designs of some of the components are considered and their advantages and disadvantages are discussed. The entire system is designed by combining these stages, and its performance is analyzed. Finally, a folded model of the system is presented.

2. OVERALL SYSTEM DESCRIPTION

The HRI-HMD inserts a small area of the high-resolution image on a large field of the low-resolution image. Using eye tracking information, the system dynamically places the high-resolution insert at the gaze point. Thus, in principle, the HRI-HMD visually provides the user with both high-resolution imagery and a large field of view. Several methods that may differ in accuracy can be used to track eye movements and the gaze points.[19,20] In order to determine the gaze point just for superposing the high-resolution insert, the required accuracy can be much lower than those provided by commercial eye trackers. Once the gaze point is determined, the superposition of the high-resolution insert over the low-resolution

background is carried out using liquid crystal devices and fixed optical components. This will result in a low cost, reliable system. To implement some of the complex human-computer interaction methods using the gaze point, the required accuracy must be in the same order as those provided by commercial eye trackers.

The schematic diagram of the HMD is shown in Figure 1. There are two displays: one for the background and the other for the insert. The image of the insert display is optically duplicated to fill the entire background display, and a liquid crystal device array is used to select one element of the array. This means that only one copy of the insert display image passes through the liquid crystal array, and all the other copies are blocked. The images of the insert display and the background display are then combined using a beam splitter.

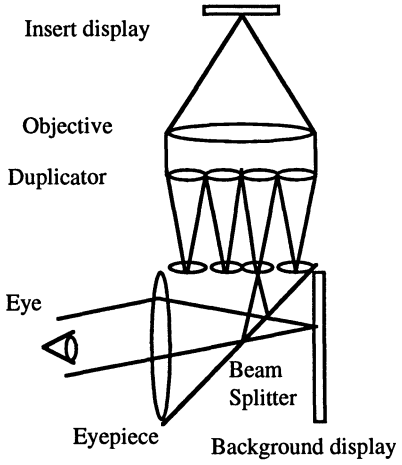

Figure 1. Schematic diagram of the HMD.

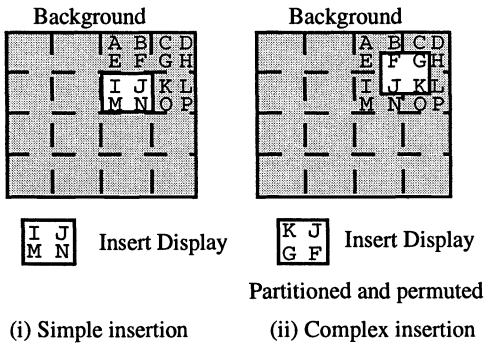

Figure 2. Superposition of the insert display.

More specifically, the light from the insert display is collimated by the objective. The collimated light is divided and focused by the duplicator to a set of identical images of the insert display, and the chief rays from these image points are set parallel to the optical axis. An array of liquid crystal shutters placed at the duplicator passes only one of these images and blocks the other images. These duplicated images are placed symmetrically to the background display with respect to the beam splitter so that the eye can see the superposed image through the eyepiece. The diagram represents the objective with a single lens, the duplicator with two arrays of lenses, and the eyepiece with another single lens.

The superposition of the insert and the background is depicted in Figure 2. In this figure, the shaded areas correspond to the background and the bright areas correspond to the insert. The character symbols represent contents of the image, and the dashed lines represent the cell boundary of the duplicated images. For a simple system, the insertion may be made at these discrete non-overlapping cell locations. In this case, the liquid crystal array may be placed anywhere inside the duplicator and blocks all the duplicated images except for one copy. When the insert image of "I J M N" is desired at a particular cell location, as shown in Figure 2-(i), this image can be directly displayed from the insert display. The duplicated images of "I J M N" fill every cell, and the copy of this image at that cell location exits the duplicator to be superposed with the background. For a complex system, the insertion may be made at continuous locations (up to the pixel level of the liquid crystal array). However, the size of the insert must be no larger than the size of a single duplicated image. In this case, the liquid crystal array must be placed near the duplicated image plane and blocks all the duplicated images except for some portions of up to four copies. When the insert image of "F G J K" is desired at a particular location, as shown in Figure 2-(ii), this image may be partitioned and permuted to "K J G F", and this transformed image can be displayed from the insert display. The duplicated images of "K J G F" fill every cell, and the portions of the four adjacent copies at that location which form the image of "F G J K" exit the duplicator to be superposed with the background.

3. PARAXIAL LAYOUT

The main component of the high-resolution insert is an optoelectronic system for duplicating the insert image and bringing the image to the eye. The basic configuration of this component is shown unfolded in Figure 3. In this figure, the rightmost

element is the insert display and the leftmost element is the eye. The first stage is the objective which collimates light from the display. The second stage is an array of telecentric systems which duplicate the display image from the collimated light and set the chief rays from the duplicated images parallel to the optical axis. We call this array of telecentric systems the duplicator, which is represented by two arrays of lenses. The third stage is the eyepiece which produces collimated light at the eye pupil from the duplicated image.

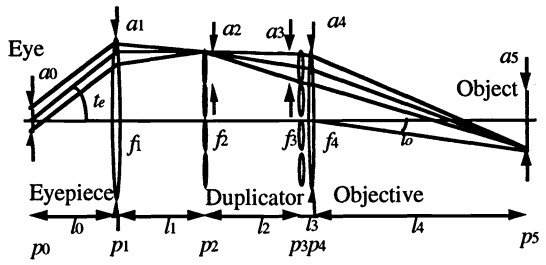

Figure 3. System parameters.

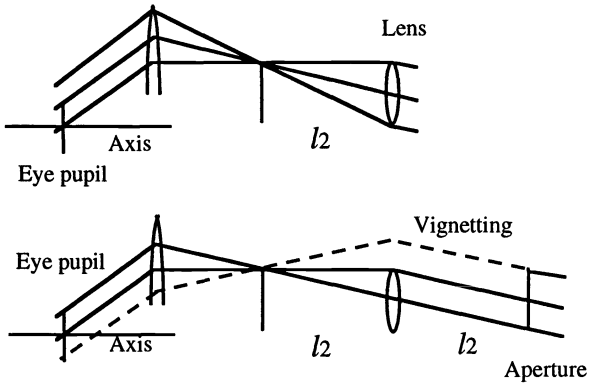

Figure 4. Duplicator in two other configurations.

To clarify the principles, an ideal thin-lens paraxial model of the system was first derived. In this ideal model shown in Figure 3, $p_0, p_1, ..., p_5$ represent planes along the optical system. More specifically, the eye pupil resides at p_0 and the display object at p_5. The eyepiece uses a lens with focal length f_1 placed at p_1. The intermediate object at p_2 is viewed by the eye placed at p_0.

The telecentric system used in the duplicator uses two lenses with focal lengths f_2 and f_3 placed at p_2 and p_3, respectively. Collimated beams at p_3 are imaged at p_2. The use of the second lens array in the duplicator is to align the principal rays parallel to the optical axis, so that they reach the axis at the eye pupil. However, this array introduces not only an additional alignment challenge but also a possible visual quality problem. This lens array must be placed at or very close to the intermediate image plane, and any scratches or dust on its surfaces significantly degrade the image quality. Furthermore, the lens boundaries may introduce an annoying blocking effect. An alternative is thus to defocus slightly the lens close to the intermediate image plane. Another alternative is to suppress that lens, as shown in Figure 4. In this figure, the second lens array is removed in both the upper and lower diagram. In addition, in the upper diagram the aperture stop is placed at the first lens array so that all rays reach the eye pupil plane, but the principal ray misses the axes at the eyepoint. In the lower diagram, however, the aperture stop is placed away from the first lens array, so that the principal ray is parallel to the optical axis between the two lenses and thus hits the axis at the eyepoint. The tradeoff, however, is that some rays do not reach the eye pupil plane due to their vignetting.

The objective uses a lens with focal length f_4 placed at p_4. Beams from the display object at p_5 are collimated at p_4.

Let's denote the distance between planes p_i and p_{i+1} and the diameter of the aperture at p_i by l_i and a_i, respectively, and the number of duplicated images along the vertical or horizontal axes, by k. The largest chief ray angle at the eye pupil is denoted by t_e, and the largest angle of the insert object subtended at the apex of the objective lens is denoted by t_o. These two parameters play essential roles in the ideal model described. From the first order constraints of the system, the relationships among these design parameters were derived in our previous paper.[18] The following summarizes these relationships:

$$f_1 = l_0 = l_1 \quad , \tag{1}$$

$$l_0 \tan t_e = \frac{k\, a_2}{2} \quad , \tag{2}$$

$$f_2 = f_3 = l_2 \quad , \tag{3}$$

$$l_2 \tan t_o = \frac{a_2}{2} \quad , \tag{4}$$

$$f_4 = l_4 \quad , \tag{5}$$

$$l_4 \tan t_o = \frac{a_5}{2} \quad , \tag{6}$$

$$\frac{a_0}{a_3} = \frac{l_1}{l_2} \quad , \tag{7}$$

$$a_3 = a_2 \quad . \tag{8}$$

	Background	Insert
Field	50° x 40°	12.5° x 10°
Pixels	640 x 480	640 x 480
Resolution	4.69 arc minutes 13 pixels/degree	1.17 arc minutes 51 pixels/degree

Table 1 : Basic design parameters

i	a_i	f_i	l_i
0	10.000	-	35.577
1	43.180	35.577	35.577
2	8.295	29.511	29.511
3	8.295	29.511	--
4	33.180	49.808	49.808
5	14.000	-	-

Table 2 : Prototype parameters [mm]

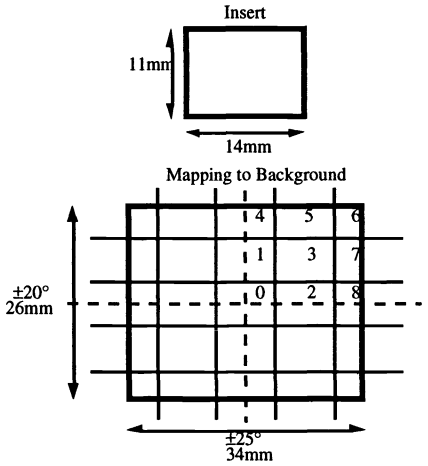

Figure 5. Mapping of the insert to the background.

The displays to be used are two active-matrix liquid crystal displays from Kopin.[22] The insert employs a 0.75" display and the background employs a 1.7" display. Both displays are in VGA standard and have 640x480 pixels. The field of view and resolution provided by these displays are summarized in Table 1. The insert image is demagnified into one-sixteenth of the background image, as shown in Figure 5. The insert display is of size 14x11 mm, and the background display is of size 34x26 mm. The area of the background display is partitioned into 25 non-overlapping cells. The insert display is optically mapped into one of these cells for superposition. There are 3x3 full-insert cells, 12 half-insert cells at both the horizontal and vertical edges, and 4 quarter-insert cells at the corners. The cells at the upper right quadrant are numbered from 0 to 8. The other quadrants are symmetrical to this quadrant, and the performance at those quadrants is equal to that at this quadrant.

The following parameter values are determined from the display devices and other design choices:

a_0 = 10 mm, a_5 = 14 mm, t_e = 25°, k = 4.

Furthermore, the value for ka_2 must be set approximately to 34 mm. When the field angle of the objective t_o is set to 8°, this value becomes 33.18 mm as computed using equation (4) and a value of 4 for k. The other parameter values are also determined and are listed in Table 2. These parameters are used to design each stage of the high-resolution insert system.

4. OPTICAL DESIGN AND ANALYSIS

In order to minimize the construction cost of the prototype, several design choices are made. The prototype design assumes monochromatic light. It is further limited to the use of identical elements in the duplicator. Nevertheless, extensions for using polychromatic visible light as well as individually optimizing elements in the duplicator are discussed. The system was designed using an optical design tool, Zemax from Focusoft.[21]

The eyepiece is designed using spherical lenses made of BK7 glass. The difficulty in designing the eyepiece is to satisfy three requirements. First, it must provide enough room for a beam splitter to be placed before the object plane. Second, the principal rays must be set parallel to the optical axis at the object plane. Finally, the field curvature at the object plane must be kept low. Simply satisfying the first two requirements gives large field curvature and astigmatism. To reduce positive field curvature, a negative lens may be placed at the object plane. However, the first and second requirements cannot be satisfied in this case. Thus, these three requirements must be traded for each other.

An initial design of the eyepiece using four lenses is shown in Figure 6-(i). There is a lot of room for a beam splitter. However, its performance suffers from all types of aberrations, as indicated in the rayfan plot in Figure 6-(ii). Consequently, the MTF plot of this design shows the highest resolvable frequency to be around 40 line-pairs/mm. This value just matches the required spatial frequency, which is calculated as 320 line-pairs in 8.295 mm (see Table 2), thus yielding 39 line-pairs/mm.

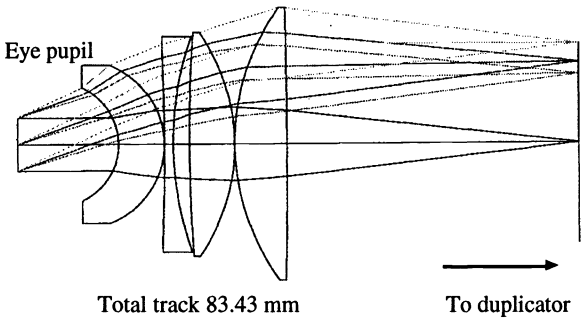

Figure 6-(i). Eyepiece layout (I).

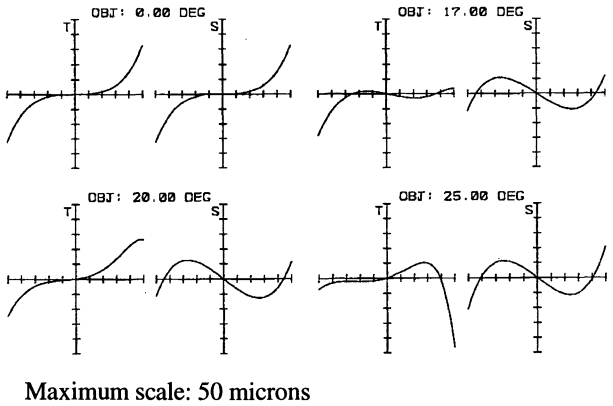

Figure 6-(ii). Eyepiece rayfan (I)

To increase the resolvable frequency of the eyepiece, two alternative designs are considered. The first alternative is to assume a curved object plane, as shown in Figure 7-(i).

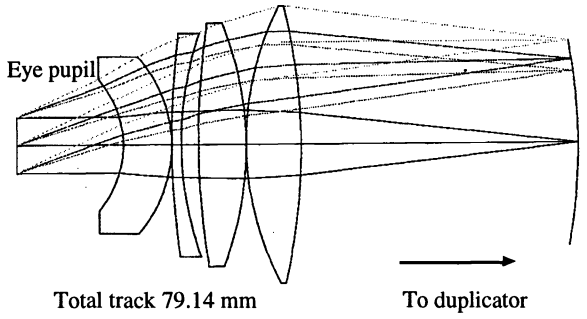

Figure 7-(i). Eyepiece layout (II).

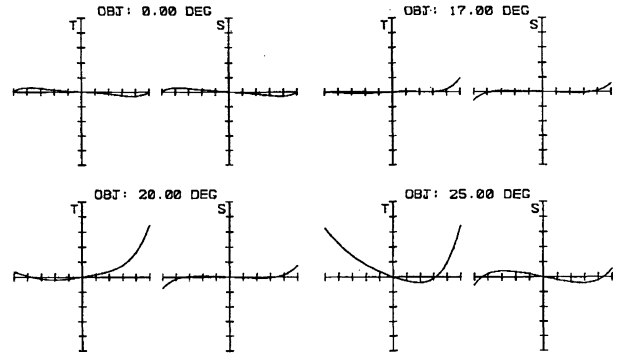

Figure 7-(ii). Eyepiece rayfan (II).

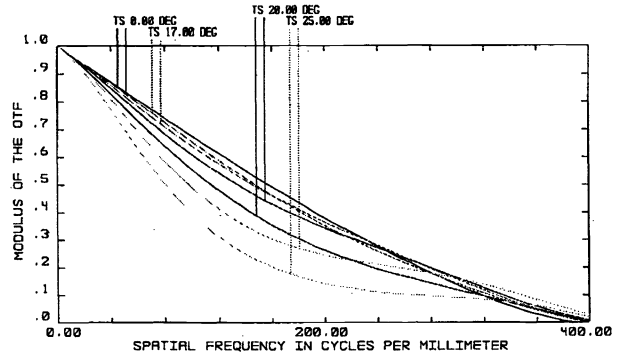

Figure 7-(iii). Eyepiece MTF (II).

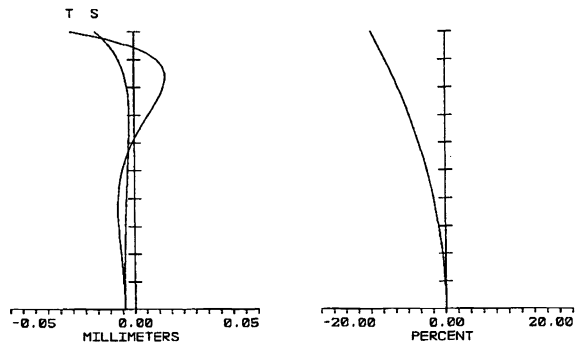

Figure 7-(iv) Eyepiece field curvature and distortion.

The object plane forms a curvature with radius of 80 mm. In this design, almost all aberrations can be removed except for astigmatism, as indicated in Figure 7-(ii) and 7-(iv). The resolvable spatial frequency of this design is much higher, as shown in Figure 7-(iii). In this design, the field angle can be increased to 35° without degrading the performance. This implies that the field of view can be increased up to 70°. A further increase in the field angle shortens the distance to the object plane and makes it difficult to place a beamsplitter within the eyepiece. To take advantage of this design, the duplicator may be designed to form the intermediate images on this curvature. The displacement of the insert images must be accompanied with a similar displacement of the background image so that they will both lie on the same curvature. This can be done by placing a negative lens right in front of the background display.

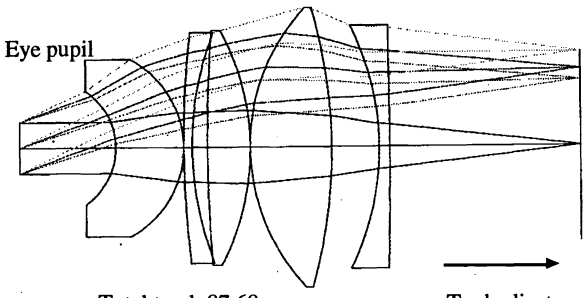

Figure 8-(i). Eyepiece layout (III).

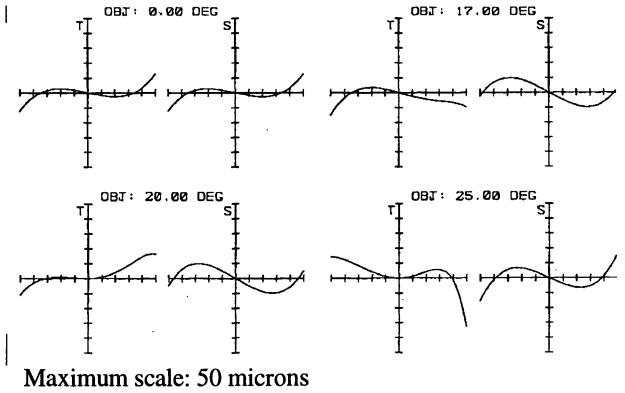

Figure 8-(ii). Eyepiece rayfan (III).

The second alternative design is to insert a negative lens between the right most lens and the object plane, as shown in Figure 8-(i). The aberrations are slightly reduced from the initial design, as shown in Figure 8-(ii), and the resolvable spatial frequency is found to be greater or equal to about 40 line-pairs/mm at 20% modulation as shown in Figure 8-(iii). For the design of the entire system, the latter is used so that each element of the duplicator can be made identical to keep the fabrication cost low.

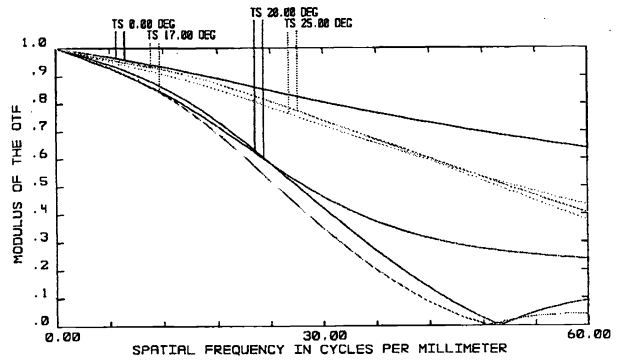

Figure 8-(iii). Eyepiece MTF (III).

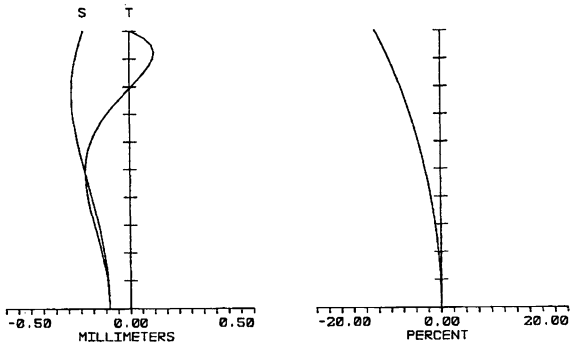

Figure 8-(iv). Eyepiece field curvature and distortion (III).

As discussed in section 3, the duplicator would typically use two lenses, one close to the objective lens and one close to the intermediate image plane, to yield an unvignetted, telecentric system. However, it was pointed out that image quality may be altered in this case. To explore those different tradeoffs, the duplicator is presented in three different forms. The first form uses spherical lenses placed at the one side or in the middle, as shown in Figure 9-(i). The second form uses spherical lenses placed at its both ends, as shown in Figure 10-(i). Their performance is shown in Figures 9-(ii) and 10-(ii), respectively. Although it is not shown in those figures, there is vignetting in both duplicators, due to the actual size of the image plane. The first form has better performance but introduces larger vignetting than the second form. The main disadvantage of these two approaches, however, is a possible alignment problem due to the need to use several lens arrays. The third form is an

alternative that uses binary optics to replace the lens arrays. The use of binary optics to fabricate an entire array on a single substrate solves the problem of aligning lenses in the arrays. However, the minimum feature size determined by the fabrication facility limits the smallest F/# of the lens to be fabricated. For analytic binarization, the minimum feature size occurs at the edges of the lens.[23] Starting with the grating equation, the definition of the F#, and the assumption that the feature size is small compared to the lens diameter and the focal length, one can derive the minimum feature size p to be given by :

$$p = \frac{\lambda}{m}\sqrt{1 + (2F/\#)^2} \quad , \tag{10}$$

where λ is the wavelength, m the number of phase levels.

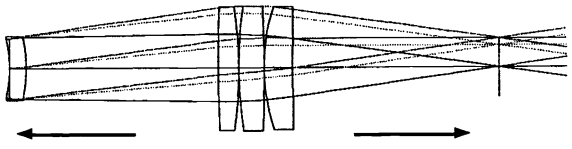

Total track 78.15mm

Figure 9-(i). Duplicator layout (I).

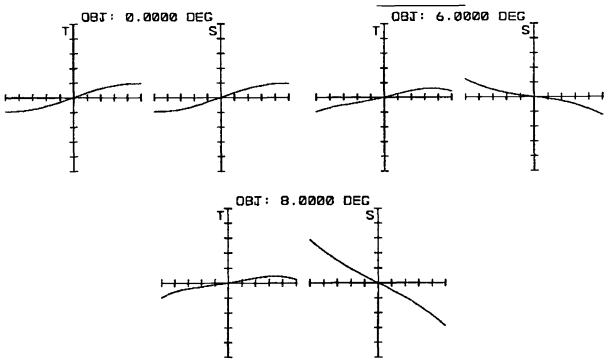

Maximum scale: 20 microns

Figure 9-(ii). Duplicator rayfan (I).

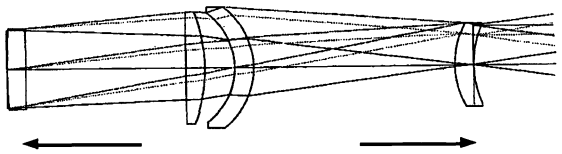

Total track 59.06 mm

Figure 10-(i). Duplicator layout (II).

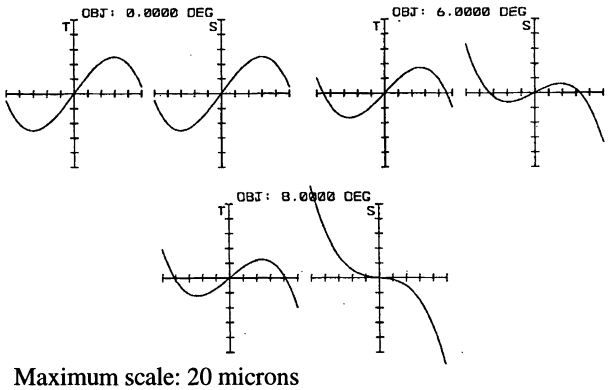

Maximum scale: 20 microns

Figure 10-(ii). Duplicator rayfan (II).

The number of phase levels must be sufficiently large in order for the fabricated lens to have high efficiency. The F/# of the duplicator is 3.6. When m = 4 levels are assumed, the minimum feature size p becomes 1 micron for wavelength 0.55 micron. An element with this feature size can be easily fabricated, since there is no alignment nor fabrication problem. In this case, an element with one binary optics surface can be designed. However, the theoretical efficiency of the lens at its edges is limited to 81%.[23] To have higher efficiency at the expense of an increase in fabrication cost, the number of phase levels can be increased. When m = 8 levels are used, p becomes 0.5 micron. At this time, the efficiency becomes 95%. However, this minimum feature size may be difficult to achieve for some facility. In order to reduce this requirement, the power of this element can be distributed in more than one surface. Using two surfaces with 95% efficiency, the efficiency of the element is kept at 90%. The design given in Figure 11-(i) uses two binary optic surfaces in SILICA and the minimum feature size is set to 1 micron. Figures 11-(ii) and 11-(iii) show its rayfan plot and MTF. The required spatial frequency at the duplicator is 39 line-pairs/mm. The layout and performance of a single binary optics element is identical to that of this

element. As it can be seen from the three layouts of the duplicator, there is some vignetting when the aperture/field diameter of the system is bounded by the image plane size. The amount of vignetting becomes largest for a single lens placed between the aperture and the image plane and possibly smaller when another lens is placed at the image plane. The paraxial models of these situations are shown in Figures 3 and 4.

The objective uses spherical lenses. Its design is shown in Figure 12-(i), and its performance is shown in Figures 12-(ii) and 12-(iii). The required spatial frequency is 23 line-pairs/mm, which corresponds to 320 line-pairs in 14 mm. The objective and duplicator form an imaging pair for the high resolution insert (see Figure 3), and thus by optimizing each element of the duplicator, the optical aberrations contributed by the objective can be reduced. More specifically, the pupil of the objective can be divided into blocks that correspond to the pupils of the duplicator. Each element of the duplicator can be optimized to reduce the aberrations of its corresponding block in the objective.

The layout for the entire system is shown in Figure 13-(i). The system is folded at several places to keep the center of gravity low and close to the head. Figures 13-(i) and 13-(ii) show the performance of the entire system at several duplicator positions, indexed from 0 to 8 according to Figure 5. These figures show that the system is capable of resolving the spatial frequency well above the required level except at the largest field angle. For a larger field of view system, the performance of the system could be improved by optimizing the eyepiece and the objective along with the duplicator, as discussed above.

The fabrication cost of a binary optics element mainly comes from a set of masks used to etch the patterns. For m phase levels, log m masks are required. The cost of a mask is proportional to its area. Thus, making non-identical duplicator elements would increase the prototype fabrication cost by several factors. However, the same mask can be repeatedly used to mass produce the same element. Binary optics has the opposite chromatic aberrations as refractive optics. Because of this property, for a compact system, binary optics is often used in conjunction with conventional refractive optics to reduce chromatic aberrations. Currently, chromatic focal shifts of the eyepiece and objective are about ± 0.5 mm for wavelength between 0.486 and 0.658 microns. In contrast, that of the duplicator using binary optics is ± 4 mm. This large chromatic focal shift is due to the fact that a large power is solely introduced by binary optics. To balance chromatic aberrations from the objective and the duplicator, some power must be introduced by refractive optics at the duplicator to reduce the influence of binary optics. However, this approach will introduce the same alignment problem as before in the lens array approaches.

5. CONCLUSION

A novel high-resolution insert HMD, named the HRI-HMD was designed and its performance was analyzed. The HRI-HMD uses only optoelectronic devices and no mechanical devices. The apparent benefit of the HRI-HMD is its potential for providing a large-field, high-resolution image, in addition to being portable. The additional benefit is its potential for supporting various gaze point oriented interaction methods. The principles of the HRI-HMD was described by formalizing the relationship among its design parameters, and the design tradeoffs were investigated from simulation.

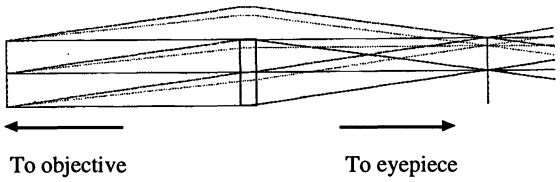

Total track 59.22 mm

Figure 11-(i). Duplicator layout (III).

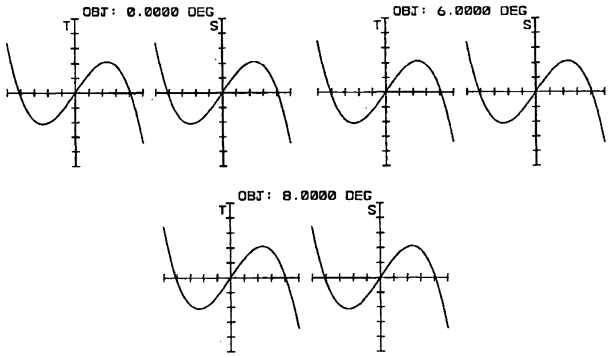

Maximum scale: 20 microns

Figure 11-(ii). Duplicator rayfan (III).

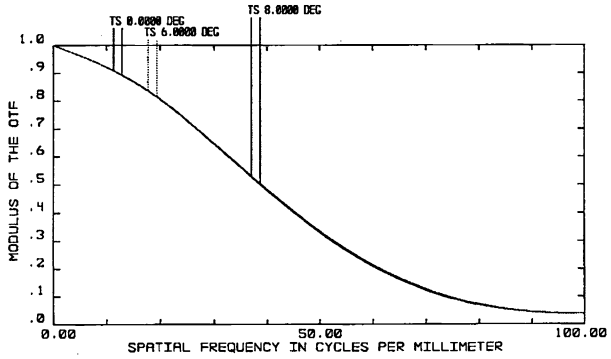

Figure 11-(iii). Duplicator MTF (III).

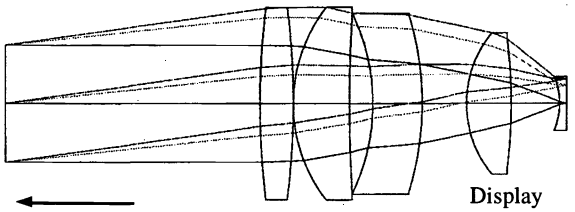

Total track 162.88 mm

Figure 12-(i). Objective layout.

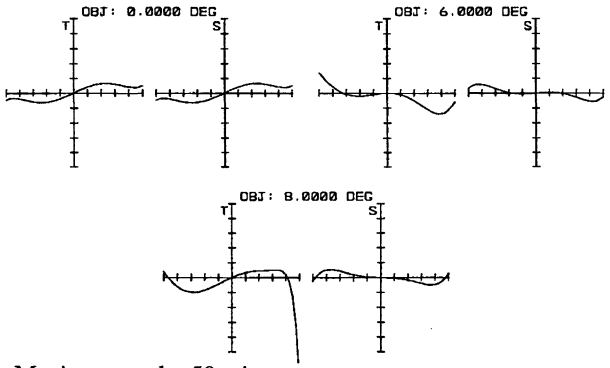

Maximum scale: 50 microns

Figure 12-(ii). Objective rayfan.

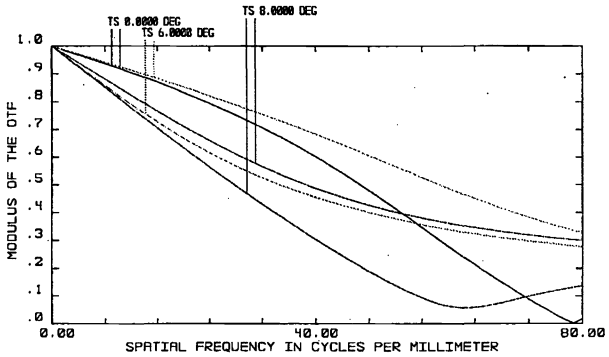

Figure 12-(iii). Objective MTF.

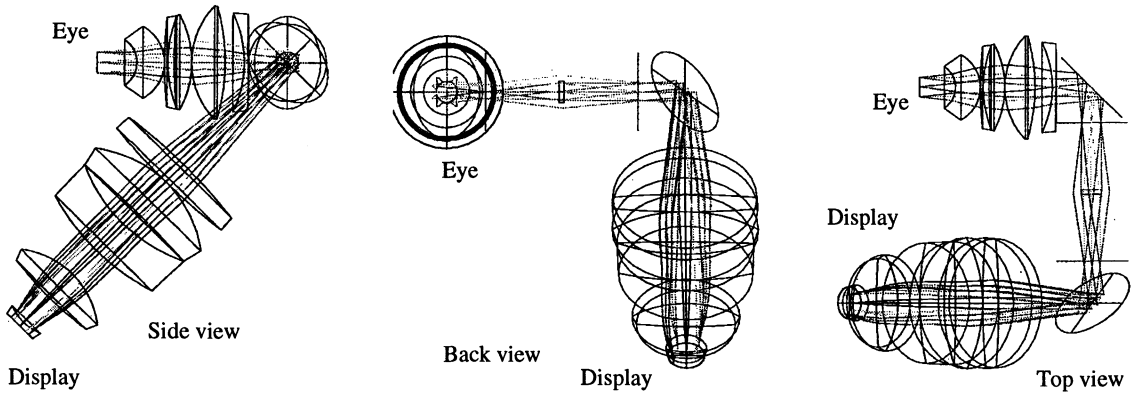

Figure 13-(i). Entire system layout.

6. ACKNOWLEDGMENTS

The authors thank Reinhardt Männer and Steffen Noehte at the University of Mannheim for their interesting discussions and equipment support, and Hudson Welch at Digital Optics Corporation for his assistance with binary optics specification and fabrication.

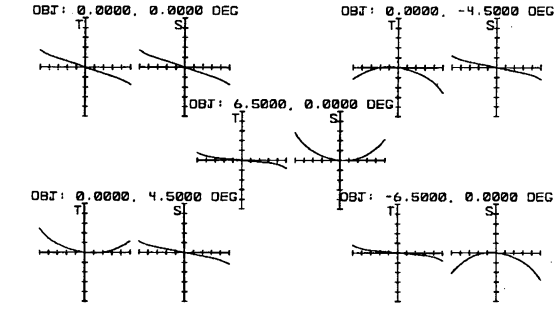

Maximum scale: 50 microns Position 0

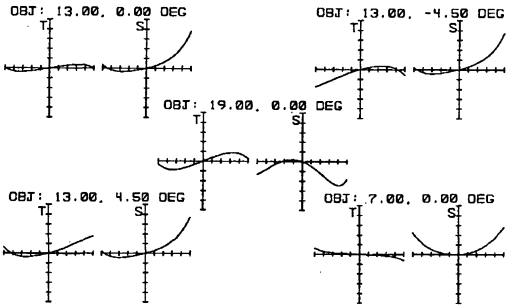

Maximum scale: 50 microns Position 2

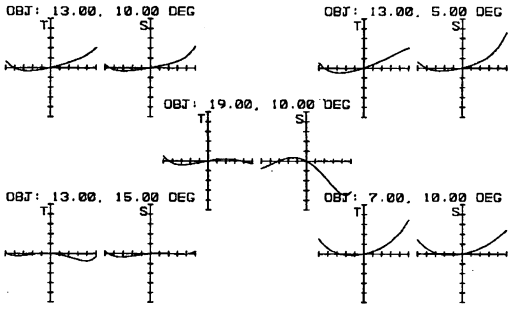

Maximum scale: 50 microns Position 3

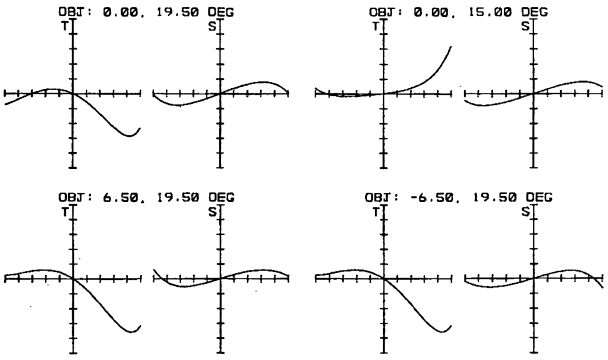

Maximum scale: 50 microns Position 4

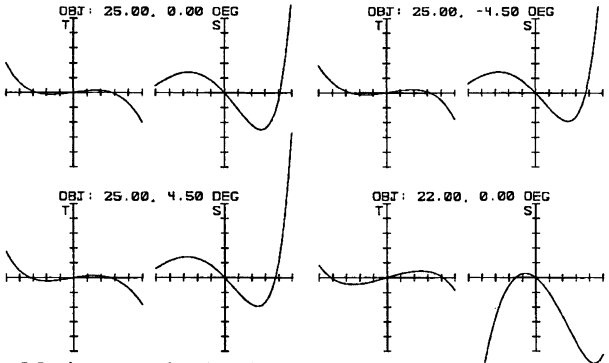

Maximum scale: 50 microns Position 8

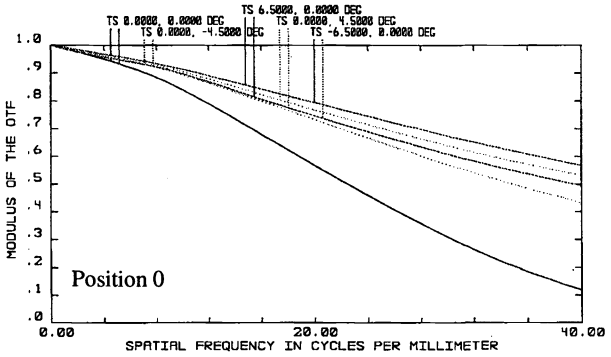

Figure 13-(ii). Entire system rayfan at several positions.

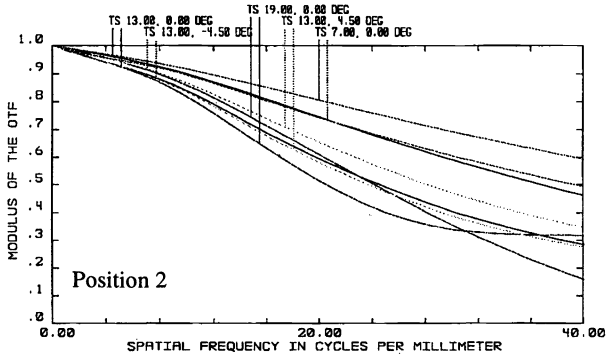

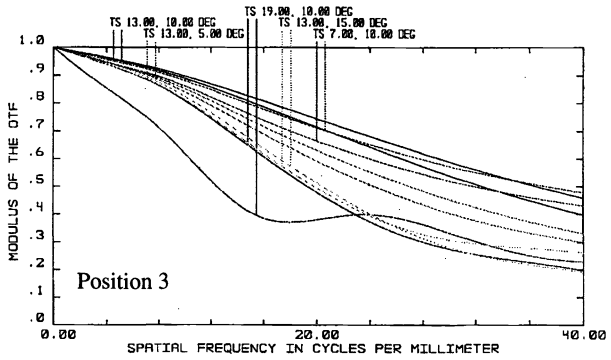

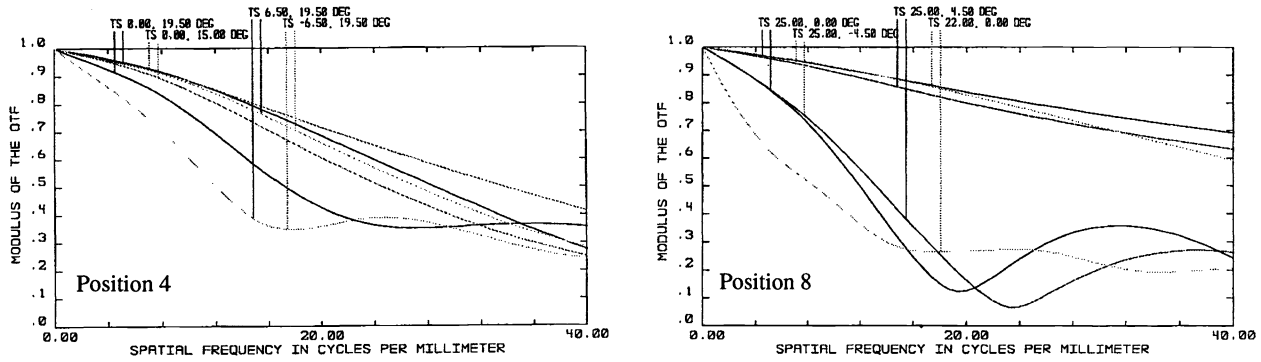

Figure 13-(iii). Entire system MTF.

7. REFERENCES

1. S. S. Fisher, "Virtual interface environments," in The Art of Human-Computer Interface Design, B. Laurel ed. (Addison-Wesley, Menlo Park, CA, 1990), pp.423-438.
2. D. Foley, "Interfaces for Advanced Computing," Scientific American 257(4), 126-135 (1987).
3. G. Burdea and P. Coiffet, Virtual Reality Technology, (Wiley & Sons, New York, NY, 1994).
4. R. E. Cole, C. Ikehara, and J. O. Merritt, "A low cost helmet-mounted camera/display system for field testing teleoperator tasks," Proc. SPIE Vol. 1669, 228-235 (1992).
5. S. S. Fisher, M. McGreevy, J. Humphries, and W. Robinett, "Virtual environment display system," ACM Workshop on Interactive 3D Graphics, Oct 23- , Chapel Hill, North Carolina (1986).
6. S. S. Fisher, M. W. McGreevy, J. Humphries, and W. Robinett "Virtual interface environment for telepresence applications," in Proceedings of the ANS International Topical Meeting on Remote Systems and Robotics in Hostile Environments, J. D. Berger, ed. (1987).
7. C. Herot, "Spatial management of data," ACM Trans. Database Systems 5(4), 493-514 (1980).
8. D. Thalmann, Using virtual reality techniques in the animation process, in Virtual Reality Systems, R. A. Earnshaw, M. A. Gigante, and H. Jones ed. (Academic Press, Reading, MA, 1993).
9. J. C. Chung, M. R. Harris, F. P. Brooks, H. Fuchs, M.T. Kelley, J. Hughes, M. Ouh-young, C. Cheung, R. L. Holloway, and M. Pique, "Exploring virtual worlds with head-mounted displays," Proc. SPIE Vol. 1083, 42-52 (1989).
10. E. M. Howlett, "High-resolution inserts in wide-angle head-mounted stereoscopic displays," Proc. SPIE Vol. 1669, 193-203 (1992).
11. H. Yamaguchi, A. Tomono, and Y, Kobayashi, "Proposal for a large visual field display employing eye movement tracking," Proc. SPIE Vol. 1194, 13-20 (1989).
12. H. Davson, Physiology of the eye, 5th ed. (Pergamon Press, New York, 1990).
13. R. A. Moses, Adlers Physiology of the eye, The C.V. Mosby Company (1970).
14. G. Westheimer, The eye as an optical instrument, in Handbook of Perception and Human Performance Vol I., 4 (Wiley-Interscience, New York, NY, 1986).
15. D. Burbidge and P. M. Murray, "Hardware improvement to the helmet mounted projector on the visual display research tool (VDRT) at the Naval Training Systems Center," Proc. SPIE Vol. 1116, 52-60 (1989).
16. M. L. Thomas, W. P. Siegmund, S. E. Antos, and R. N. Robinson, "Fiber optic development for use on the fiber optic helmet mounted display," Proc. SPIE Vol. 1116, 90-101 (1989).
17. F. J. Ferrin, "Survey of helmet tracking technologies," Proc. SPIE Vol. 1456, 86-94 (1991).
18. A. Yoshida, J. P. Rolland, and J. H. Reif, "Design and applications of a high-resolution insert head-mounted-display," Proc. of the IEEE Virtual Reality Annual International Symposium, 84-93 (1995).
19. Applied Science Laboratories, Eye tracking systems handbook, (Applied Science Laboratories, Waltham, MA, 1992).
20. L. Young and D. Sheena, "Survey of eye movement recording methods," Behavior Research Methods, Instruments and Computers Vol. 7, 397-429 (1975).
21. Focusoft, Zemax optical design program user's guide ver. 3.0, (Pleasanton, California 94566, 1994).
22. J.P. Salerno, "Single Crystal Silicon AMLCDs," International Workshop on Active Matrix Liquid Crystal Displays, 14th International Display Research Conference, 1-7, (1994).
23. J. Jahns, "Diffractive optical elements for optical computers," in Optical Computing Hardware, J. Jahns and S. H. Lee, ed. (Academic Press, Boston, MA, 1994), pp. 137-167.